Doklady Earth Sciences, Vol. 373, No. 5, 2000, pp. 855–858. Translated from Doklady Akademii Nauk, Vol. 372, No. 5, 2000, pp. 683–686.

GEOPHYSICS

Different Regimes of the Geomagnetic Field Generation During the Last 165 Ma

M. Yu. Reshetnyak and V. E. Pavlov

Presented by Academician V.N. Strakhov January 5, 1999

Received January 14, 1999

There is a detailed picture of the geomagnetic field polarity behavior for the last 165 Ma [1]. The distribution of temporal field inversions is characterized by the existence of an extensive zone with a constant polarity, which is often related to a new regime of the geomagnetic field generation, in the Cretaceous. At present there exist numerous contradictory statements and interpretations of the geodynamo theory from this standpoint (see the review [2]). Therefore, using the model of αω-dynamo as an example, we attempted to perform a consecutive analysis of possible regimes of the geomagnetic field generation and examine the correlation between regularities in the distribution of field intensity inversions, processes in the Earth's liquid core, and processes in the *D*" layer. A comparatively new statistical method, namely, the wavelet-analysis [3], was used for analyzing evolutionary characteristics of the geomagnetic polarity scale (GPS).

The process of geomagnetic field inversions can be described in the framework of determinate solutions of the MHD equations in partial derivatives. The number of unknowns in these equations exceeds two. Therefore, at a supercritical value of the parameter responsible for the convection intensity, the (magnetohydrodynamic) MHD equations can have random solutions. This statement is in compliance with the observation of inversions [4]. The described determinate mechanism of inversions does not rule out the "catastrophic" mechanism of inversions based on the cardinal rearrangement of currents in the liquid core [5, 6], however, in our opinion, it seems to be simpler and does not require any external influences. Without going into the fine structure of inversion distribution and its evolution, the GPS as a whole can be described in terms of fractals (see, for instance, [7, 8]) reflecting the ideas of self-similarity.

Since the geodynamo processes are closely connected with the core–mantle thermal regime, convection in the mantle, and, in particular, the thermal boundary layer *D*" [9], it would be logical to expect a modulation of these processes that is expressed in the existence of periodicities in the number of inversions, field intensity, etc. The application of a comparatively new spectral method, the wavelet-analysis [3], has proved to be convenient for analyzing nonstationary temporal sequences. This method allows us to analyze both the data with omissions [10] and the piecewise continuous functions, such as the signal of geomagnetic polarity [11]. By definition, the wavelet-transformation of the time series $f(t)$ is specified by the relationship

$$w(a, t) = a^{-3/2}\int \psi\left(\frac{t'-t}{a}\right) f(t')dt',$$

where a is the scale parameter, $\psi(t)$ is the analyzing wavelet, whose choice depends on the problem being solved; the coefficient before the integral is chosen in such a way that w is proportional to the number of magnetozones with the duration a. The Morle wavelet $\psi(t) = e^{-t^2/2}e^{2\pi it}$ having a good spectral resolution is used in this work.

Figure 1 illustrates the evolution of the spectrum $\log(w(a, t))$ for the polarity signal of the type 0…0…1…1 with the step $\Delta t \sim 10^4$ yr. Note that the geomagnetic field polarity signal was for the first time analyzed in the work [11], where the polarity signal spectrum was shown to be connected with other characteristics of the field, for instance, its intensity. The obtained spectrum demonstrates the absence of distinct periodicities, probably with the exception of the process with $a \sim 25$ Ma for the 20–130 Ma time interval. The wavelet-diagram may be arbitrarily divided into four regions: A (118–165 Ma), B (25–83 Ma), C (0–25 Ma), and D (83–118 Ma). Regions A and C represent the intervals with the continuously filled spectra; region B is characterized by a large inhomogeneity of the spectrum in the range of small scales ($a < 1$ Ma); and finally, region D represents the interval of the superchron.

Figure 2 depicts the dispersion

Schmidt Joint Institute of Physics of the Earth (OIFZ), Russian Academy of Sciences, Bol'shaya Gruzinskaya ul. 10, Moscow, 123810 Russia

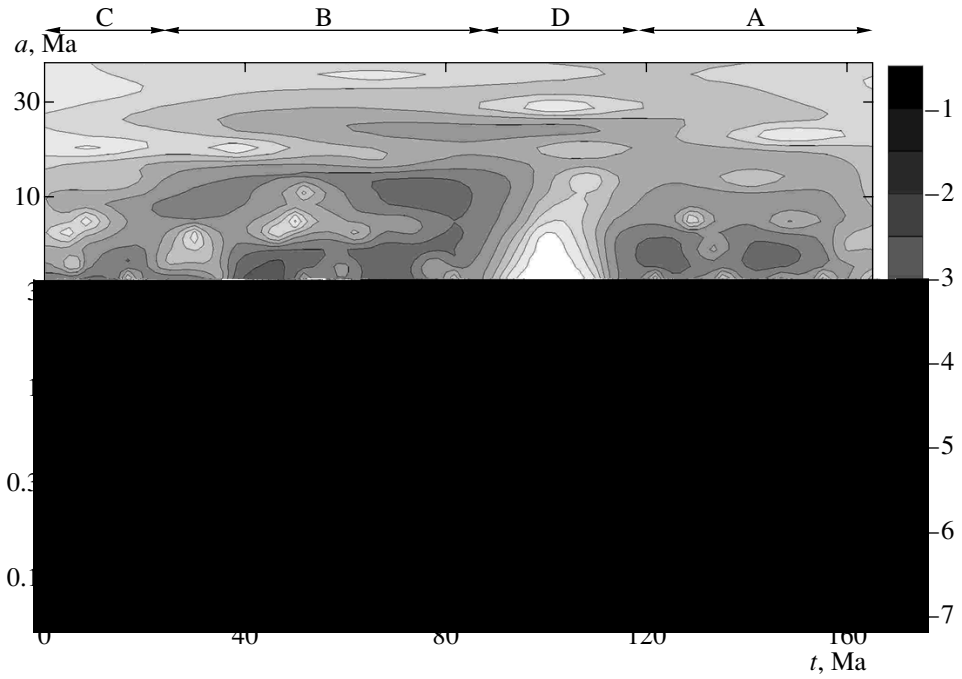

Fig. 1. Wavelet-transformation $\log(w(a, t))$ of the polarity signal.

$$\sigma(a) = \frac{1}{t_2 - t_1}\int_{t_1}^{t_2}(\log(w(a, t)) - \log(\overline{w(a)}))^2 dt,$$

where $\overline{w(a)} = \frac{1}{t_2 - t_1}\int_{t_1}^{t_2} w(a, t)dt$ is the average (in time) for the three regions A, B, and C. The behavior of dispersions is characterized by two regimes. The first regime is small-scale ($a < 1$ Ma): all three plots have approximately the same slope; however, the dispersion value for interval B after the superchron exceeds the dispersion values for quiet regions A and C by a factor of 2–3. The second regime has $a > 1$ Ma; here, the dispersion weakly depends on a and does not undergo any noticeable changes during the superchron passage. Hence, at small time scales ($a < 1$ Ma), the GPS spectrum contains information regarding the superchron after the superchron interval as well. Note that the characteristic time of the memory (the duration of interval B) about the superchron (D) substantially exceeds not only the characteristic magnetohydrodynamic times (~10^4 yr) but also the duration of the superchron itself (D).

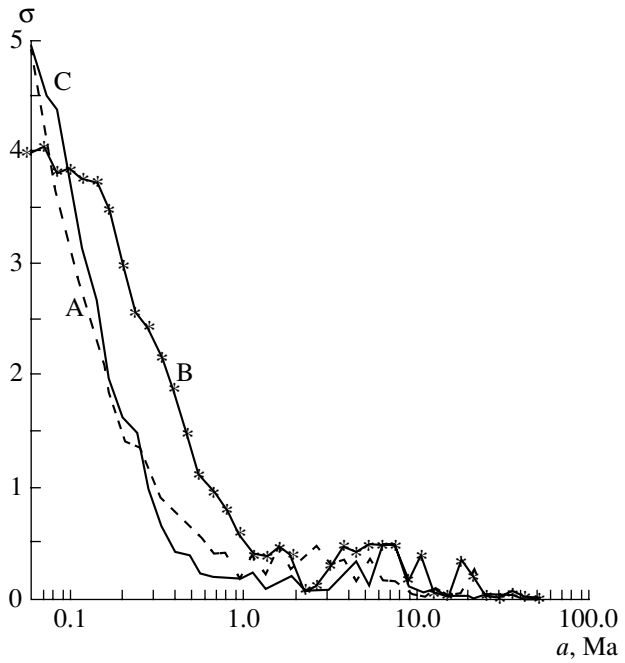

Fig. 2. Dependence of dispersion $\sigma(a)$: (A) 118–165 Ma; (B) 25–83 Ma; (C) 0–15 Ma.

It should be remembered that the conclusion on the similarity of regions A and C in the GPS was also made in [12] on the basis of analyzing the durations of magnetozones with a constant polarity. However, the obtained similarity should be regarded with caution. Since the information concerning the field polarity does not reflect the whole state of the geodynamo system, additional characteristics of the field must be used. As such, we considered the behavior of the geomagnetic field paleointensity taken from the work [13] and presented in Fig. 3. It clearly follows from the figure that the modern field intensity (interval C) exceeds its characteristic value up to the superchron (A) more than twice. Let us turn to geodynamo theory fundamentals for possible interpretation combining the similar behavior of spectra and paleointensity.

From the standpoint of long-period characteristics of the field, the αω-models of geodynamo are best stud-

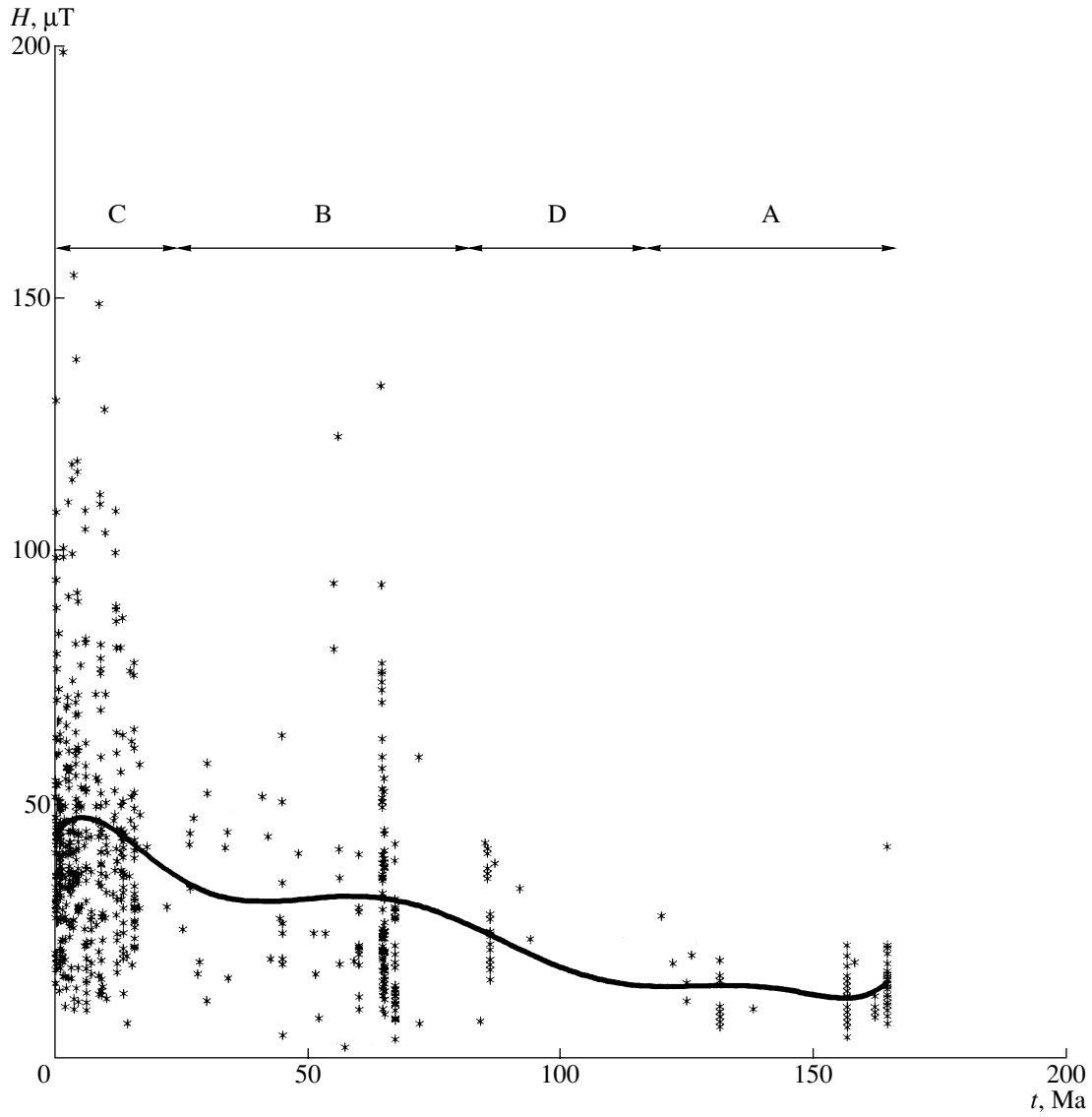

Fig. 3. Evolution of the paleointensity.

ied (see, for instance, [14]). The solution properties depend on the dimensionless amplitudes of α- and ω effects:

$$R_\alpha = \frac{\alpha L}{\eta_m + \eta_t}, \quad R_\omega = \frac{\Omega' L^2}{\eta_m + \eta_t},$$

where $\alpha = \tau\langle v \operatorname{rot} v\rangle/3$; L is the dimension of the convective shell; Ω is the angular velocity of the differential rotation; η_m and η_t ($\sim lv/3$) are the coefficients of molecular and turbulent magnetic diffusions; τ ($\sim l/v$), l, and v are the time of the turbulent vortex revolution, its spatial scale, and the velocity amplitude, respectively. The generation threshold in the approximation of αω-models, where $R_\alpha^2 \sim R_\omega$, depends on the amplitude of the dynamo-number $\mathcal{D} = R_\alpha R_\omega$. For universally accepted distributions of the α effect, the critical dynamo-number is $\mathcal{D}_0 \approx 5600$. There is reason to believe that the $\mathcal{D}$ sign determining the motion direction of dynamo-waves is positive for the Earth: the waves move from the equator poleward [14]. At $\mathcal{D} > \mathcal{D}_0$, the solution is at first periodic (with the period $T_0 \sim 10^4$ yr) and has a zero average in time. Since the field alters its polarity during each such oscillation, we can identify these oscillations with frequent inversions. With the $\mathcal{D}$ increase (≈14000), a new mode with a nonzero average appears in the solution [14]. This regime corresponds to the regime without inversions. A further increase of the $\mathcal{D}$ value ($\mathcal{D} > 36\,000$) leads to the bifurcation of the third mode, and the solution becomes chaotic; inversions appear again. The R_α and R_ω values in turn depend on the regime of the thermal flux at the core–mantle boundary and the regime of the *D*" layer.

Considering, as a first approximation, the linear dependence of Ω and v on the buoyancy Θ, which is proportional to the temperature gradient deviation from the adiabatic value, in the Earth's liquid core, we have the following dependence:

$$\mathcal{D} \sim \frac{\Theta^2}{(C+\Theta)^2},$$

where $C \sim \eta_m$. Since $\eta_t \sim \eta_m$ [15], both of the terms in the denominator are of the same order of magnitude, and, as can be easily verified, at small changes of Θ $\mathcal{D} \sim \Theta$. The Θ value in turn depends on the state of the thermal boundary layer *D*". The presence of the stable boundary layer results in a heat emission decrease and in convection weakening. Since the boundary layer itself can be convective, and due to convection in the core and lower mantle, the layer can decay (possibly locally), reducing the temperature at the external core boundary by the jump value in the layer (~10^3 °C) and thereby increasing convection. Without regard for convection in the *D*" layer, the evaluation of the characteristic time for the thermal signal transit through the layer yields $\sim\delta^2/k = 10^2$ Ma, where $\delta = 10^2$ km is the *D*" layer thickness, $k = 4 \times 10^{-6}$ m^2 s^{-1} is the coefficient of its thermodiffusion. The introduction of convection into *D*" can reduce the characteristic times of processes. These thermal instabilities in *D*" can modulate geodynamic processes and can be recorded as changes in inversion frequencies, paleointensity values, and dispersion in the geomagnetic field direction.

In accordance with these notions, one can propose the following scenario for the geodynamo process during the last 165 Ma. Within interval A, the system was in a weakly excited state $\mathcal{D} < 14000$ with a small field intensity. At this moment, the *D*" layer had the greatest thermal conductivity, and, accordingly, the thermal flux through the layer was minimum. Further, partial destruction of the *D*" layer occurred that resulted in the convection intensity increase ($\mathcal{D} > 14\,000$). The latter led to the bifurcation in the solution of induction equation for the magnetic field and to the appearance of a new mode with a nonzero average. This state (D) is characterized by the complete absence of inversions and a field paleointensity increase. The next two intervals (B and C) reflect the further destruction of the *D*" layer and correspond to the state with an increased intensity of convection and field. Note that, according to [14], the intensity increase is proportional to $\sqrt{\mathcal{D}}$. The beginning of interval B coincides with the appearance of chaotization in the solution ($\mathcal{D} > 36\,000$) and is characterized by increased dispersion. As a result of the convection intensity increase, the "chaotic" mode amplitude grows and becomes comparable with the amplitude of the mode with the nonzero average in time, and inversions become frequent again (interval C).

In conclusion, it should be noted that the considered scenario is not unique. The analysis based on $\alpha^2\omega$-models, which unfortunately are less studied at present, can serve as an alternative scenario.

ACKNOWLEDGMENTS

The authors are grateful to D.K. Galyagin and P.G. Frik for a complex of programs on the wavelet-analysis, as well as to D.D. Sokolov for useful discussions.

This work was supported by the Russian Foundation for Basic Research, project nos. 97-05-64797 and 07-05-64798, as well as by the INTAS, project no. 348 (1999).

REFERENCES

1. Opdyke, N.D. and Channell, J.E.T., *Magnetic Stratigraphy*, San Diego: Academia, 1996.
2. Jacobs, J.A., *Reversals of the Earth's Magnetic Field*, Cambridge: Cambridge Univ. Press, 1994.
3. Holschneider, M., *Wavelets: An Analysis Tool*, Oxford: Oxford Univ., 1995.
4. Cox, A., *J. Geophys. Res.*, 1968, vol. 73, pp. 3247–3253.
5. Olson, P., *Phys. Earth Planet. Int.*, 1983, vol. 33, pp. 260–274.
6. Kalinin, Yu.D., *Geomagn. Aeron.*, 1986, vol. 26, pp. 358–359.
7. Pecherskii, D.M., Reshetnyak, M.Yu., Sokolov, D.D., and Kheida, P., *Geomagn. Aeron.*, 1998, vol. 38, no. 4, pp. 132–142.
8. Ivanov, S.S., *Geomagn. Aeron.*, 1994, vol. 33, no. 5, pp. 181–189.
9. Loper, D.E., *Geophys. Res. Lett.*, 1982, vol. 19, no. 1, pp. 25–28.
10. Galyagin, D.K. and Frik, P.G., *Matemat. Model. Sistem Protsessov*, 1996, no. 4, pp. 10–19.
11. Galyagin, D.K., Reshetnyak, M.Yu., Sokolov, D.D., and Frik, P.G., *Dokl. Akad. Nauk*, 1998, vol. 67, p. 123–129.
12. Gallet, Y. and Hulot, G., *Geophys. Res. Lett.*, 1997, vol. 24, no. 15, pp. 1875–1878.
13. Perrin, M. and Shcherbakov, V., *J. Geomag. Geoelectr.*, 1997, vol. 49, pp. 601–614.
14. Pecherskii, D.M., Reshetnyak, M.Yu., Sokolov, D.D., and Kheida, P., *Geomagn. Aeron.*, 1998, vol. 38, no. 4, pp. 108–117.
15. Anufriev, A.P., Reshetnyak, M.Yu., and Sokolov, D.D., *Geomagn. Aeron.*, 1997, vol. 37, no. 5, pp. 141–146.